Colloid Polym Sci 280:336–341 (2002)

ORIGINAL CONTRIBUTION

J. M. Ruso
David Attwood
P. Taboada
V. Mosquera

Self-association of *n*-hexyltrimethylammonium bromide in aqueous electrolyte solution

Received: 4 June 2001
Accepted: 17 September 2001

J. M. Ruso · P. Taboada · V. Mosquera
Grupo de Física de Coloides y Polímeros
Departamento de Física Aplicada y
Departamento de Física de la Materia
Condensada, Facultad de Física
Universidad de Santiago de Compostela
15706 Santiago de Compostela, Spain

D. Attwood (✉)
School of Pharmacy and Pharmaceutical
Sciences, University of Manchester
Manchester M13 9PL, UK
e-mail: david.attwood@man.ac.uk
Tel.: +44-161-2752328
Fax: +44-161-2752396

Abstract The self-association of *n*-hexyltrimethylammonium bromide (C_6TAB) in aqueous solution has been studied by static and dynamic light scattering and NMR spectroscopy at 25 °C in the presence of added electrolyte, and critical aggregation concentrations, aggregation numbers and the degree of ionization have been calculated. Aggregation numbers determined from light scattering and from the application of mass-action theory to the concentration dependence of ^{1}H NMR chemical shifts of four protons along the alkyl chain of C_6TAB, were between three and four over the range of electrolyte concentration studied (0.2–0.7 molkg^{-1} NaBr). A structure for the small aggregates has been proposed from the NMR chemical shift data.

Keywords *n*-Hexyltrimethyl ammonium bromide · Micelles · Electrolyte effect on self-association

Introduction

The association properties of the *n*-alkyltrimethylammonium bromide series (C_nTAB) of surfactants have been extensively studied. Changes in the size [1–4], shape [5–7] and ionization [8] of the C_nTAB series with an increase in the hydrocarbon chain length from eight to 16 have been reported. Zielinski et al. [9, 10] reported the adiabatic compressibilities and apparent molar volumes of octyl-, decyl-, dodecyl-, and tetradecyltrimethylammonium bromides. De Lisi et al. [11] measured the thermodynamic properties of nonyl- and decyltrimethylammonium bromides. In previous work [12–14] we investigated the micellar behaviour of C_nTAB with $n = 8$, 10, 12, and 14 in different media and at several temperatures to gain information on the effect of pH and alkyl chain length on the thermodynamics of micellization of these surfactants. In a recent study [15] we extended the work on the C_nTAB series by measurements of the physicochemical properties of aqueous solutions of C_6TAB. The critical aggregation concentration (cac) and counterion binding were determined from conductivity and ultrasound velocity measurements at temperatures between 15 and 45 °C and in a range of electrolyte concentrations up to 0.6 molkg^{-1} NaBr. In addition, apparent adiabatic compressibilities were calculated from a combination of ultrasound velocity and density measurements. The results of this study led to the suggestion of very small aggregates with a highly organized core and a high degree of exposure of the associated components to the aqueous environment.

In the present study we extend our investigation of the association properties of C_6TAB with particular emphasis on the influence of electrolyte on aggregate size and ionization. A possible structure for the C_6TAB aggregate is proposed from measurements of the chemical shift of selected protons on dilution using NMR techniques.

Experimental

Materials

C_6TAB was obtained from Lancaster Synthesis. Water was double-distilled, deionized, and degased before use. Sodium bromide (Fluka) was of analytical grade. Solutions for the NMR studies were prepared in 99.93% deuterium oxide (Sigma-Aldrich, UK).

Light scattering measurements

Static light scattering measurements were made at 25 ± 0.1 °C using a Malvern 7027 laser light scattering instrument equipped with a 2-W argon ion laser (Coherent Innova 90) operating at 488 nm with vertically polarized light. The solutions were clarified by ultrafiltration through 0.1-μm filters with the ratio of light scattering at angles of 45° and 135° not exceeding 1.10. The refractive index increments of C_6TAB were measured at 25 ± 0.1 °C using an Abbé 60/DE precision refractometer (Bellingham and Stanley). Measurements over the range of electrolyte concentration showed no effect of electrolyte on the value of the refractive increment within the limits of the error of the measurement.

Dynamic light scattering measurements were made at 25 ± 0.1 °C at a scattering angle of 90° with the Malvern instrument described earlier combined with a Brookhaven BI 9000AT digital correlator with a sampling time range of 25 ns to 40 ms. The solutions were clarified as described previously. The diffusion coefficients were determined from a single-exponential fit to the correlation curve. The hydrodynamic radii were calculated from measured diffusion coefficients by means of the Stokes–Einstein equation.

NMR spectroscopy

^{1}H NMR spectra were recorded using a JEOL EX270 270 MHz spectrometer at 20 ± 0.1 °C. The chemical shifts of selected peaks were accumulated using a peak-pick facility. All spectra were compared with sodium 3-(trimethylsilyl)propionate, which acted as an internal standard.

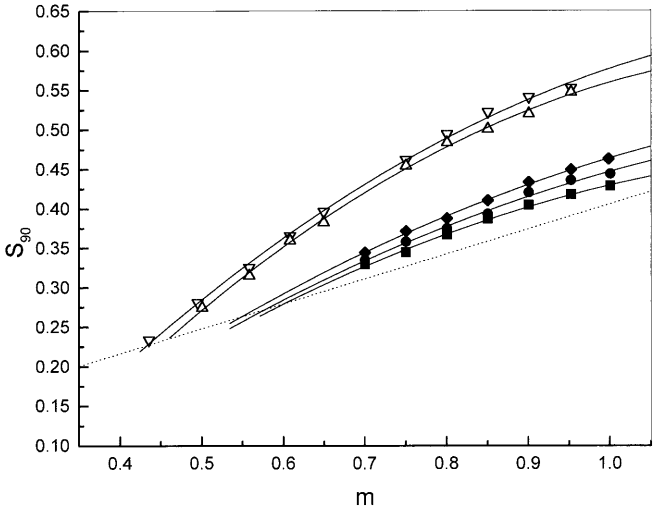

Fig. 1 Variation of the scattering ratio, S_{90}, with concentration, m, for n-hexyltrimethylammonium bromide (C_6TAB) in aqueous NaBr solutions of concentrations of 0.2 molkg^{-1} (*squares*), 0.3 molkg^{-1} (*circles*), 0.4 molkg^{-1} (*diamonds*), 0.5 molkg^{-1} (*up triangles*), and 0.7 molkg^{-1} (*down triangles*) at 25 °C. Monomer line (—)

Table 1 Aggregation properties of n-hexyltrimethylammonium bromide (C_6TAB) in aqueous electrolyte solution at 25 °C from static light scattering. Estimated uncertainties: critical aggregation concentration (*cac*), aggregation number (N) and αÿ ± 20%

[NaBr] (molkg^{-1})	cac (molkg^{-1})	N	α	ΔG^0_m (kJmol^{-1})
0.2	0.61	3	0.4	−17.6
0.3	0.58	3	0.5	−17.2
0.4	0.55	3	0.5	−17.3
0.5	0.46	4	0.5	−17.8
0.7	0.43	4	0.6	−17.5

Results and discussion

Static light scattering

The variation of the intensity of light scattered from a solution at 90° relative to the scattering from benzene (S_{90}) is shown in Fig. 1 as a function of the n C_6TAB concentration, m, at electrolyte concentrations between 0.2 and 0.7 molkg^{-1} NaBr.

The cac, corresponding to the intersection of the scattering curve and the theoretical line representing ideal scattering from monomers (shown by a dashed line in Fig. 1), are given in Table 1. The cac values are higher than those previously determined by ultrasound velocity techniques [15], most probably as a consequence of the differently weighted averages from these techniques that become significant for the weakly associating, polydisperse systems under investigation. The aggregation numbers, N, and effective micelle charges, z, were calculated according to the Anacker and Westwell [16] treatment, in which the light scattering from solutions of ionic aggregates is represented by

$$\frac{K'm_2}{\Delta R_{90}} = \frac{2m_3 + N^{-1}\left(z+z^2\right)m_2}{[2N + 2N^{-1}(z+z^2)f^2 - 2fz]m_3 + zm_2} \quad , \qquad (1)$$

where ΔR_{90} is the Rayleigh ratio of the solution in excess to that of a solution at the critical concentration, m_2 is the molality of the aggregated species in terms of monomer, m_2 is the molality of the supporting electrolyte (including free monomer), and $f = (\mathrm{d}n/\mathrm{d}m_3)_{m_2}/(\mathrm{d}n/\mathrm{d}m_2)_{m_3}$. K' for vertically polarized incident light is defined by

$$K' = 4\pi^2 n_0^2 (\mathrm{d}n/\mathrm{d}m_2)^2_{m_3} V^0/L\lambda^4 \quad , \qquad (2)$$

with n_0 being the refractive index of the solvent (water or aqueous NaBr containing surfactant at the cac), V^0 the volume of solution containing 1 kg water, L Avogadro's number, and λ the wavelength of the incident light (488 nm). Expansion of Eq.(1) in powers of m_2 leads to

$$\frac{K'm_2}{\Delta R_{90}} = A + Bm_2 + \cdots \quad , \tag{3}$$

where

$$A = 4N\left[(2N - fz)^2 + zf^2\right]^{-1} \tag{4}$$

and

$$B = zA(2m_3)^{-1}\left[(1+z)N^{-1} - A\right] \quad . \tag{5}$$

An aggregation number of 3 was determined previously by light scattering for C_6TAB in water [15]. Although the micellar parameters calculated by this treatment should be regarded with caution in view of the possible errors associated with application of this theory to systems of such low aggregation number, the results of Table 1 nevertheless serve to show a minimal influence of electrolyte concentration over the range 0–0.7 molkg^{-1} NaBr. This behaviour is in contrast with that of the short-chain anionic surfactant sodium hexyl sulphate (SHS) [17], the aggregation number of which, as calculated by the same theoretical treatment of light scattering data, increases from 3 to 8 with an increase in electrolyte concentration over the range 0–0.5 molkg^{-1} NaCl.

Values (per mole of monomer) of the standard Gibbs energy change on aggregate formation, ΔG^0_m, were calculated from the following expression [18], assuming that the self-assembly of these molecules may be described using the mass-action model,

$$\Delta G^0_m = (2-\alpha)RT \ln X_{cac} \quad , \tag{6}$$

where X_{cac} is the critical aggregation concentration expressed as a mole fraction (including bromide ions from the free monomers) and α is the degree of ionization ($\alpha = z/N$). Table 1 shows no consistent change in ΔG^0_m with electrolyte concentration as might be expected from the lack of aggregate growth with electrolyte addition.

Dynamic light scattering

The apparent diffusion coefficients, D, of C_6TAB in water and aqueous electrolyte solutions are presented in Fig. 2 as a function of the aggregate concentration, m_2. The experimental data were fitted with the linear function

$$D = D_0\left(1 + k'_D m_2\right) \quad , \tag{7}$$

where D_0 is the limiting diffusion coefficient. Measurements of the apparent diffusion coefficients of surfactants with a high cac may be strongly influenced by the presence of monomers that produce a rapid increase in D in the vicinity of the cac. To avoid this potential source of error, measurements were restricted to a concentration in which D was a linear function of molality [19, 20]. Hydrodynamic radii, r_h, were derived from the limiting diffusion coefficients using the Stokes–Einstein relationship:

$$r_h = \frac{k_B T}{6\pi\eta D_0} \quad , \tag{8}$$

where k_B is the Boltzmann constant, T the temperature, and η the solvent viscosity. Table 2 shows only a slight increase of hydrodynamic radius as a function of added salt concentration, in agreement with the minimal effects of electrolyte on aggregation number. It is of interest to compare these results with the effects of electrolyte on the size of SHS aggregates [17]. These two C_6-chain surfactants have identical r_h (and N) values in 0.2 molkg^{-1} electrolyte; however, the hydrodynamic radius of SHS increased by 32% with an increase in electrolyte concentration to 0.5 molkg^{-1} compared to only 17.5% for C_6TAB, in line with corresponding changes in aggregation number ($N = 8$ for SHS in 0.5 molkg^{-1} NaCl).

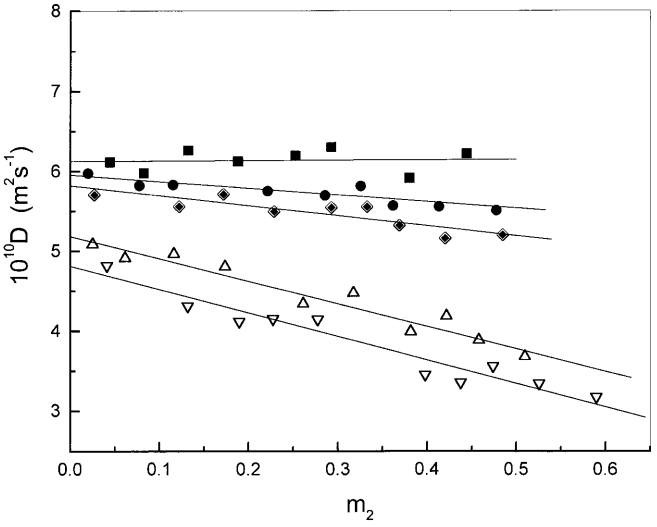

Fig. 2 Diffusion coefficient, D, as a function of the aggregate concentration for C_6TAB in aqueous NaBr solutions of concentrations of 0.2 molkg^{-1} (*squares*), 0.3 molkg^{-1} (*circles*), 0.4 molkg^{-1} (*diamonds*), 0.5 molkg^{-1} (*up triangles*), and 0.7 molkg^{-1} (*down triangles*) at 25 °C

Table 2 Limiting diffusion coefficient, D_0, and hydrodynamic radius, r_h, of C_6TAB in aqueous electrolyte solution at 25 °C. Estimated uncertainties: D_0 and r_h ± 5%

[NaBr] (molkg^{-1})	10^{10} D_0 (m^2s^{-1})	r_h (nm)
0.2	6.12	0.40
0.3	5.96	0.41
0.4	5.82	0.42
0.5	5.19	0.47
0.7	4.81	0.51

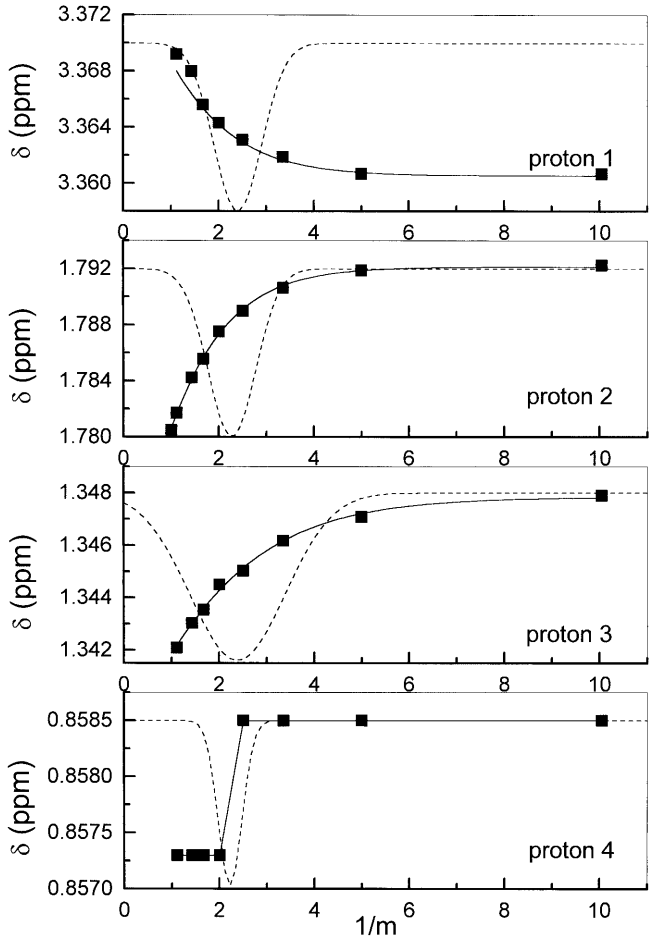

Fig. 3 Variation of the ^{1}H chemical shift for the four selected protons of the C_6TAB molecule as a function of the reciprocal concentration in 0.5 molkg^{-1}NaBr. The *dashed lines* represent the Gaussian fit of the second derivative derived as outlined in the text

NMR spectroscopy

The self-association of C_6TAB was further investigated by high-resolution NMR spectroscopy. ^{1}H NMR spectra of C_6TAB solutions at a range of concentrations well below and above the cac were compared at electrolyte concentrations over the range 0.0–0.5 molkg^{-1} NaBr. The assignment of the spectral lines was by comparison with literature spectra [21–24]. The chemical shifts, δ, of the four selected protons shown in Scheme 1 are plotted as a function of reciprocal concentration in Fig. 3.

A downfield shift on aggregation is noted for proton 1, with upfield shifts observed for protons 2, 3, and 4. Inflections in the plots of Fig. 3 were detected by analysis of the data using a recently developed procedure [25] based on the Runge–Kutta numerical integration method and the Levenberg–Marquardt least-squares fitting algorithm. This analytical procedure, which is of particular value in the determination of inflections in data from systems of low aggregation number, is based on the Phillips definition of the critical micelle concentration as the concentration corresponding to the maximum change in the gradient in plots of the solution chemical shift versus concentration [26]. The cac from the chemical shift data may be defined as

$$\left(\frac{\mathrm{d}^3\delta}{\mathrm{d}\,(1/m)^2}\right)_{m=\mathrm{cac}} = 0 \ . \tag{9}$$

The results of the analysis of the data of the selected protons of C_6TAB in the presence of 0.5 molkg^{-1} NaBr are shown in Fig. 3 as plots of the measured chemical shift and a Gaussian fit of its second derivative derived as outlined earlier. Similar plots were obtained for all the electrolyte concentrations studied. The values of the cac obtained by this method for each of the selected protons were similar (Table 3) and in reasonable agreement with the values from static light scattering.

An examination of the magnitude and sign of the changes of chemical shift on aggregation can provide an insight into the possible ordering of molecules in the aggregates. The upfield shifts for protons 2, 3, and 4 indicate that these protons are transferred to a more apolar environment on self-association [27]. In contrast, the downfield shift of proton 1 indicates a stronger interaction with water molecules. In typical spherical aggregates the magnitude of the chemical shift on aggregation for protons along the alkyl chain decreases with a decrease in the packing density on moving outwards from the core to the aggregate surface. This decrease in shift is a result of a decrease in the screening effect on the protons [28]. Examination of Fig. 3 shows an increase in the magnitude of the chemical shift in the order proton 4 < proton 3 < proton 2, suggesting an increase in packing density on moving outwards from the

Table 3 cac and N determined from the chemical shifts of selected protons along the alkyl chain of C_6TAB (Scheme 1). Estimated errors in N and cac are ± 1 and ± 0.05 molkg^{-1}, respectively

[NaBr] (molkg^{-1})	Proton 1		Proton 2		Proton 3		Proton 4
	cac	N	cac	N	cac	N	cac
0.0	0.61	–	0.64	–	0.63	–	0.60
0.2	0.54	2	0.59	2	0.57	–	0.57
0.3	0.54	3	0.58	2	0.54	3	0.52
0.4	0.50	3	0.54	3	0.50	4	0.49
0.5	0.40	4	0.44	5	0.42	6	0.45

centre of the aggregate, rather than inwards as in typical micelles. A suggestion for a possible arrangement of monomers, which satisfies these requirements and also ensures maximum separation of charges, is an aggregated structure formed by three (or four) monomers crossing each other in the region of their second alkyl carbons (Fig. 4). There is a high degree of exposure of alkyl chains to the aqueous solvent in such small structures, as indeed was noted from the results of our earlier study on SHS [17].

If we assume that the mass-action law is applicable to aggregates of this size, the aggregation numbers may, in principle, be derived from the chemical shift data. The chemical shift can be written [29, 30]

$$\delta_{\mathrm{obsd}} = \frac{m_2}{m}\delta_{\mathrm{m}} \quad , \tag{10}$$

where m_2 and m are the aggregate concentration and the total solute concentration respectively. δ_{obsd} is the observed chemical shift and δ_{m} the shift of aggregated solute both taken relative to the chemical shift of the monomer, determined by extrapolation to zero solute concentration. It is possible to express the concentration of monomer as

$$[A] = m\frac{\delta_{\mathrm{m}} - \delta_{\mathrm{obsd}}}{\delta_{\mathrm{m}}} \tag{11}$$

and the aggregate concentration as

$$N[A_{\mathrm{n}}] = m\frac{\delta_{\mathrm{obsd}}}{\delta_{\mathrm{m}}} \quad . \tag{12}$$

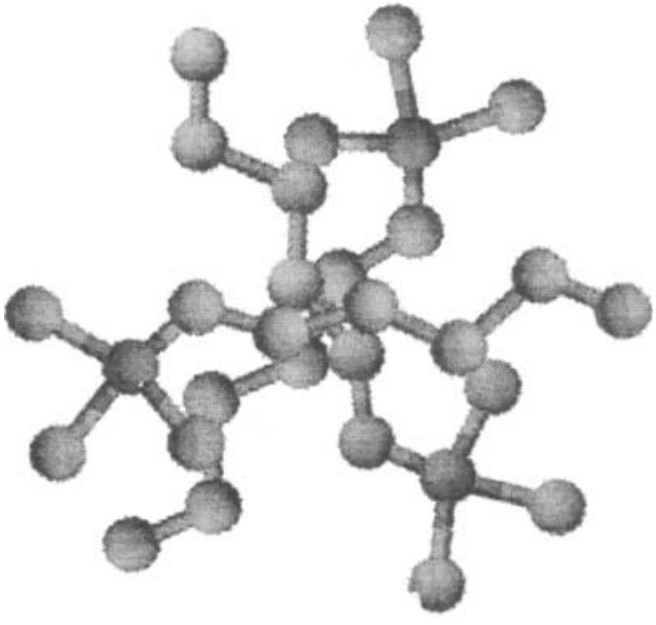

Fig. 4 Proposed structure of aggregates of C_6TAB

Then the expression for the mass-action equilibrium constant, K, is

$$\ln(m\delta_{\mathrm{obsd}}) = N\ln[m(\delta_{\mathrm{m}} - \delta_{\mathrm{obsd}})] + \ln K + \ln N - (N-1)\ln\delta_{\mathrm{m}} \quad . \tag{13}$$

Plots of $\ln(m\delta_{\mathrm{obsd}})$ against $\ln[m(\delta_{\mathrm{m}} - \delta_{\mathrm{obsd}})]$ thus yield the aggregation number and the equilibrium constant. The chemical shift data for C_6TAB in 0.5 molkg^{-1} NaBr plotted according to Eq. (13) are shown in Fig. 5. Similar plots were obtained for data in the other electrolyte concentrations studied. The aggregation numbers derived by this method using the data for protons 1–3 at each electrolyte concentration are shown in Table 3. The values obtained support the conclusions from light scattering that there is limited self-association of this surfactant.

The small size of the aggregates of C_6TAB calls into question whether these are true micelles in the accepted sense and, hence, whether we are justified in our use of a mass-action model of micellization. The presence of an inflection point in the light scattering plots of this study and those observed in conductivity and ultrasound plots of our previous study [15] support the assumption that the self-association conforms to a closed model. Moreover, the enthalpy of micellization of C_6TAB predicted by application of the mass-action model to cac data was in good agreement with the value measured directly by microcalorimetry [15]. In addition, our experience from measurements on solutions of weakly associating drugs has shown a clear distinction between those exhibiting such inflections, which behave as micellar systems, and others in which there is a continuous change in properties with concentration increase, which can be modelled by open association models [31].

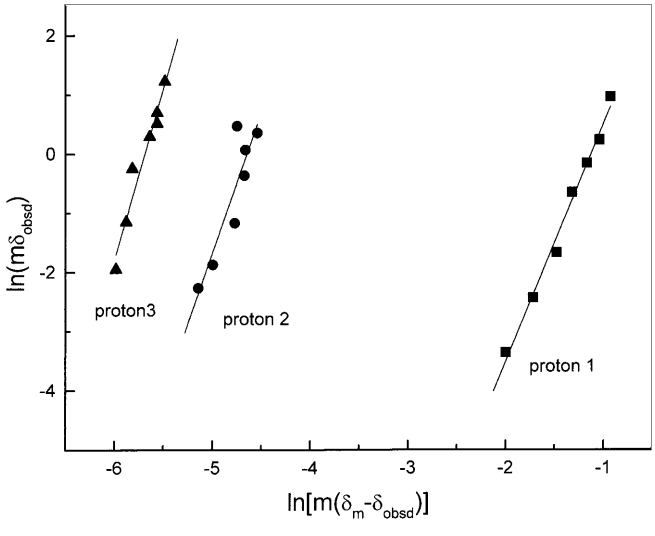

Fig. 5 NMR chemical shift data of selected protons plotted according to Eq. (13) for C_6TAB in 0.5 molkg^{-1} NaBr

Conclusion

Our study has shown that C_6TAB forms trimers or tetramers in aqueous electrolyte solution of concentration up to 0.7 $molkg^{-1}$. Measurement of chemical shifts of selected protons along the hydrophobic chain by NMR has suggested an aggregate in which monomers cross each other in the region of their second alkyl carbons, which provides maximum separation of charge but results in a high degree of exposure of alkyl chains to the aqueous solvent.

Acknowledgement This work received the financial support of the Xunta de Galicia.

References

1. Jones MN, Piercy J (1972) J Chem Soc Faraday Trans 1 68:1839
2. Dorshow R, Briggs J, Bunton CA, Nicoli DF (1982) J Phys Chem 86:2388
3. Briggs J, Dorshow R, Bunton CA, Nicoli DF (1982) J Chem Phys 76:775
4. Drifford M, Belloni L, Dubois M (1987) J Colloid Interface Sci 118:50
5. Stigter D (1967) J Colloid Interface Sci 23:379
6. Israelachvili JN, Mitchell DJ, Ninham BW (1976) J Chem Soc Faraday Trans 2 72:1525
7. Lee YS, Woo KW (1995) J Colloid Interface Sci 169:34
8. Zana R (1980) J Colloid Interface Sci 78:330
9. Zielinski R, Ikeda S, Nomura H, Kato S (1987) J Colloid Interface Sci 119:398
10. Zielinski R, Ikeda S, Nomura H, Kato S (1988) J Chem Soc Faraday Trans 1 84:151
11. De Lisi R, Ostiguy C, Perron G, Desnoyers JE (1979) J Colloid Interface Sci 71:147
12. del Río JM, Pombo C, Prieto G, Sarmiento F, Mosquera V, Jones MN (1994) J Chem Thermodyn 26:879
13. del Río JM, Pombo C, Prieto G, Mosquera V, Sarmiento F (1995) J Colloid Interface Sci 172:137
14. del Río JM, Prieto G, Sarmiento F, Mosquera V (1995) Langmuir 11:1511
15. Mosquera V, del Río JM, Attwood D, García M, Jones MN, Prieto G, Suárez MJ, Sarmiento F (1998) J Colloid Interface Sci 206:66
16. Anacker EW, Westwell AE (1964) J Phys Chem 68:3490
17. Ruso JM, Attwood D, Taboada P, Mosquera V, Sarmiento F (2000) Langmuir 4:1620
18. Moroi Y (1988) J Colloid Interface Sci 122:308
19. Turq P, Drifford M, Hayoun M, Perera A, Tabony J (1983) J Phys Lett 44:471
20. Drifford M, Belloni L, Dubois M (1987) J Colloid Interface Sci 118:50
21. Williams DH, Fleming I (1995) Spectroscopy methods in organic chemistry, 5th edn. McGraw-Hill, New York
22. Bhacca NS, Johnson LF, Shooley JN (1963) High-resolution NMR spectra catalogue, vols I and II. Varian Associates, Palo Alto
23. Pouchert CJ (1983) The Aldrich library of NMR spectra, vols 1 and 2, 2nd edn. Aldrich Chemical Company
24. Pretsch E, Clerc T, Seibl J, Simon W (1983) Tables of spectral data for structure determination of organic compounds, English edn. Springer, Berlin Heidelberg New York
25. Ruso JM, Taboada P, Attwood D, Mosquera V, Sarmiento F (2000) Chem Phys 2:1261
26. Phillips JN (1955) Trans Faraday Soc 51:561
27. Bijma K, Engberts JBFN (1997) Langmuir 13:4843
28. Yoshino A, Yoshida T, Okabayashi H, Kamaya H, Ueda I (1998) J Colloid Interface Sci 198:319
29. Persson B-O, Drakenberg T, Lindman B (1976) J Phys Chem 80:2124
30. Persson B-O, Drakenberg T, Lindman B (1979) J Phys Chem 83:3011
31. Attwood D, Florence AT (1983) Surfactant systems. Chapman and Hall, London, pp 124–228